Computational Physics & Astronomy (188B)

Project V: Spectral Analysis

Erik Lamb

March 15, 2016

1 Introduction

Spectral analysis is analysis of a periodic signal in terms of its frequencies which are related to certain important values such as energy and correlation. Whenever periodic signals in the form of data are received, it is always in the time-domain, meaning the signals are a function of time. However, various important properties of a signal can be extrapolated by analyzing a signal in the frequency-domain, where the signal is given as a function of frequency. By analyzing a signal in the frequency-domain, across a range of frequencies, we are performing *spectral analysis*. In order to conduct spectral analysis on a signal, we must first *transform* the signal from the natural time-domain to the frequency-domain. This is accomplished via famous transformations called Fourier transforms, which can convert a signal to the frequency-domain and back to the time-domain. The continuous Fourier transforms for a periodic signal $X(t)$ of period T (note that the signal must be periodic in order to perform a Fourier transform) are given by

$$\begin{aligned} \hat{X}_k &= \frac{1}{T}\int_0^T X(t)\exp(-2\pi ikt/T)dt \\ X(t) &= \sum_{k=-\infty}^{\infty} \hat{X}_k \exp(2\pi ikt/T) \end{aligned} \tag{1}$$

The first equation gives the forward Fourier transform, whereas the second equation gives the backward or inverse Fourier transform on the interval $[0, T)$. Notice that the second equation simply says that we can write the periodic signal $X(t)$ as a sum of sinusoidal waves. $\hat{X}_k$, therefore, is a complex number that defines the amplitude and phase of the wave. The index k is called the wavenumber, and it is related to the frequency of the signal $X(t)$ by the relation

$$f(k) = k/T \tag{2}$$

The first equation in Eqn. (1) technically transforms the signal $X(t)$ into k-space, but from Eqn. (2) we see that frequency-space and k-space are equivalent. For the remainder of this project. We will work in k-space when performing forward Fourier transforms.

In this project, we will be performing spectral analysis using the above methods on two sets of data given in the text files `sunspots_monthly.txt` and `rays_monthly.txt`. These data files were provided by the Royal Observatory of Belgium in Brussels and by the Oulu Cosmic Ray Station at the Sodankyla Geophysical Observatory in Finland, respectively. The file `sunspots_monthly.txt` provides the monthly mean total sunspot number and the file `rays_monthly.txt` contains the count rate of cosmic rays reaching the Earth in counts/min, corrected for pressure and efficiency and also given monthly. A sunspot is dark spot visible on the surface of the Sun which produces a very intense magnetic field and the raw number of sunspots is used to measure solar magnetic activity. Cosmic rays, on the other hand, are charged, high energy particles that originate from

outside the solar system and bombard Earth, affecting cloud formation by ionizing atmospheric particles. Because the cosmic rays are charged, they interact with magnetic fields. When the Sun is experiencing high solar magnetic activity, meaning there is a large amount of sunspots on the Sun's surface, the increased magnetic field makes it difficult for the cosmic particles to reach Earth, making the two data sets anti-correlated. This, along with other spectral analysis of these two signals, will be the focus of the this project.

As mentioned above, a signal must be periodic in order to perform spectral analysis on it. The data given in the files `sunspots_monthly.txt` and `rays_monthly.txt` constitute two signals, both with a period of $T = 50$ *years* and both with $N = 600$ data points, one for every month of every year since 1966. Because these two signals has a discrete set of data points, we cannot use Eqn. (1) directly to perform spectral analysis. Instead, we must first discretize the Fourier transforms. This is the subject of the next section where we review the methods used to produce the results.

2 Methods

As mentioned in the introduction, in order to perform spectral analysis on the discrete sunspot signal and cosmic ray signal, we must discretize the Fourier transforms given by Eqn. (1). Because there N data points taken over a period T, we can first discretize time with the time step $\Delta t = T/N$. So discretized time is given by,

$$t_n = n\Delta t \qquad for \quad n = 0, 1, 2, 3... \tag{3}$$

Having discretized time we can then discretize our signal $X(t)$ as $X(t_n) = X_n$. We can now discretize the Fourier transforms using the discrete signal in the time domain given by X_n. The final form of the discretized Fourier transforms are known as the discrete Fourier transforms or DFT. They are given by

$$\begin{aligned} \hat{X}_k &= F\{X_n\}_k = \sum_{n=0}^{N-1} X_n \exp(-2\pi ikn/N), \qquad k = 0, 1, 2, ..., N-1 \\ X_n &= F^{-1}\{\hat{X}_k\}_n = \frac{1}{N}\sum_{k=0}^{N-1} \hat{X}_k \exp(2\pi ikn/N), \qquad n = 0, 1, 2, ..., N-1 \end{aligned} \tag{4}$$

In the above equation, the forward Fourier transform of the discrete signal X_n, $\hat{X}_k$, can now only be determined over a finite frequency range given by $f_{min} = -(N/2-1)/T \leq f \leq f_{max} = (N/2)/T$, where any frequency outside of this range is mapped back to lie inside it. Since we will be working in k-space, we desire a relation between the frequency f and the wavenumber k which can be found from the frequency range and is given by,

$$f(k) = \frac{1}{T}\begin{cases} k, & 0 \leq k \leq N/2 \\ k - N, & N/2 < k < N \end{cases} \tag{5}$$

Frequency values for $N/2 < k$ are negative, but are equal in magnitude to the frequency values for $k \leq N/2$. These negative frequencies correspond to the complex conjugates of the $\hat{X}_k$ coefficients. But since our signals are real, these values of $\hat{X}_k$ for $N/2 < k$ are redundant and can be neglected for problems where our result is in k-space, such as problem one. Thus, our k will only run from 0 to $N/2 = 300$.

As mentioned earlier, by transforming our real, time-domain signal to the frequency-domain, we can reveal characteristics of our signal that are not intuitive. The power spectrum, for example, can measure the distribution of wave amplitudes of signal. More importantly the peaks of the power spectrum represent the dominant modes of a signal; frequencies which alone determine the basic shape of signal and contribute more to power and amplitude than any other frequency. Additionally,

when the power spectra is flat it indicates undesirable noise and reveals which range of frequencies are causing it. The power spectrum of a signal is written in terms of the complex coefficients $\hat{X}_k$, since the power of signal is proportional to the square of the amplitude. Thus, the power spectrum of a signal in k-space is given by

$$P_k = \frac{T^2}{N^2}|\hat{X}_k|^2 \tag{6}$$

Equation (6) will be particularly important for problem one.

We now move on to describe our last tool required for completing this project; correlation functions. A correlation function tells us how well two signals $X(t)$ and $Y(t)$ match-up when one of those signals is shifted by a time lag τ. The continuous expression of a correlation function is given by,

$$C_{XY}(\tau) = \lim_{T\to\infty}\int_0^T X(t+\tau)Y(t)^* dt \tag{7}$$

When $X \neq Y$, Eqn. 7 is called a *cross-correlation* function. When $X = Y$, Eqn. 7 is called an *autocorrelation* function. However, because our signals are discrete, so too must we discretize the correlation function given by (7). For discrete signals with N data points, the number or data points in the overlapping or corresponding region changes as the time lag between the signals is changed. In order to account for this, we must "pad" our signal with an additional N zeros. Therefore, our discrete signal X_n, for example, is now

$$\tilde{X}_n = (X_0, X_1, X_2, ..., X_{N-1}, 0, 0, ..., 0) \tag{8}$$

and similarly for Y_n. Thus, our extended or "padded" signal now has a length of $2N$. For a discrete time lag l, we can now write a discrete correlation function, given by

$$C_{XY}(l) = \frac{1}{N-|l|}\sum_{n=0}^{2N-1}\tilde{X}_{n+l}\tilde{Y}_n^* \tag{9}$$

Using the discrete Fourier transforms (DFT) given by Eqn. (4) and applying them to Eqn. 9, we achieve our desired result of a discrete correlation function written in terms of discrete Fourier transforms,

$$C_{XY}(l(n)) = \frac{1}{N-|l(n)|}F^{-1}\{F\{\tilde{X}_n\}_k \cdot F\{\tilde{Y}_n^*\}\}_n \tag{10}$$

where the discretized time lag l can be given as function of n by

$$l(n) = \begin{cases} n, & 0 \leq n \leq N \\ n-2N, & N < n < 2N \end{cases} \tag{11}$$

and positive lags are for $0 \leq n \leq N$ and negative lags are for $N < n < 2N$. Finally, as in problems two and three, we will need to first normalize our discrete signals X_n and Y_n before we pad them with zeros and apply the correlation function (10). We normalize signals with the transformation,

$$X_n \to (X_n - \overline{X})/\sigma_x \tag{12}$$

where $\overline{X}$ is the mean of the data points in X_n and σ_x is the standard deviation of the data points in X_n. A similar formula is used for Y_n. By normalizing our signals in this way we ensure that our correlation function given by (10) will be bounded between -1 and 1; $-1 \leq C_{XY}(l(n)) \leq 1$. Correlation function values of 1 indication total correlation (the signals are the same), whereas correlation function values of -1 indicate total anti-correlation (the signals are the opposite). Correlation values near 1 or -1 indicate strong correlation or ant-correlations, respectively.

Before moving on to the results a few comments must be made. First, unless otherwise stated all frequency values have units $1/year$ and all time-period values have units of $years$. Secondly, for the following results we used the Fast-Fourier Transform algorithms `irfft()`, which gives the real inverse Fourier transform, and `rfft()`, which gives the real forward Fourier transform, provided by `numpy` library `numpy.fft` in Python to implement Eqn. (4).

3 Results

3.1 Power Spectra

For this problem, we were to compute the power spectra of the sunspot and the cosmic ray signals using the data given. Recall that the power spectra of any signal is given by Eqn. (6). From (6), we found the power spectra for both signals, which is given in the frequency domain. Therefore, the power spectra are a function of the wavenumber k by the function for frequency given by Eqn. (5). Our results for the sunspot and cosmic ray signals are shown in figures 1 and 2, respectively. Note that, because both signals are real inputs, only the wavenumber values of $0 \leq k \leq N/2$ for $N = 600$ data points are required since the remaining values simply give the complex conjugates and are therefore redundant.

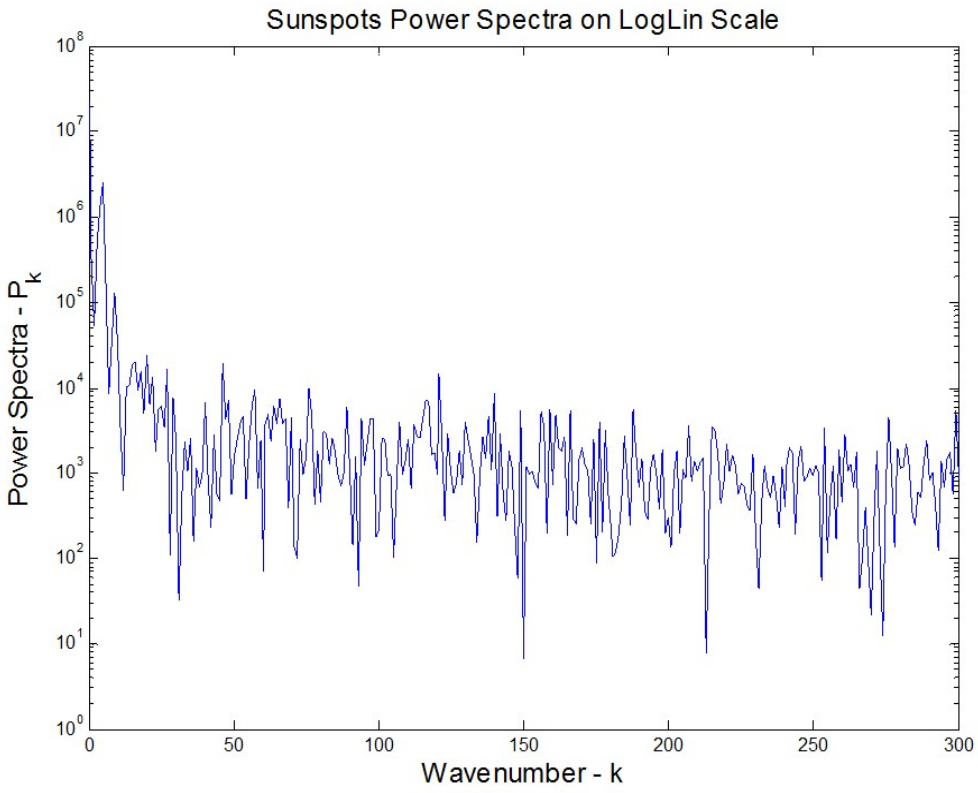

Figure 1: Sunspots signal power spectrum plot in k-space on a LogLin scale, meaning only the y-axis is on a logarithmic scale. Notice that largest non-zero spike occurs for a very low wavenumber k.

Both Fig. 1 and 2 are similar in that they have a maximum peak at $k = 0$ with successive peaks of smaller magnitude as k, and therefore the frequency, increases. From this we can infer that low-frequency signals for both the sunspots and the cosmic rays are more dominant, having larger amplitudes and therefore larger values of power than the high-frequency signals. Qualitatively this result makes sense because for $k = 0$ the dominant mode, which is the mode with the lowest cut-off frequency of all modes, of both signals is for a frequency of $f = 0\ 1/year$, which means the time period T_k of the dominant mode for both signals is $T_0 = 1/f = \infty\ years$. We would expect the amplitude, and therefore the power, of a signal that counts the number of sunspots or cosmic ray count rates observed per month to be at a maximum if the time period of those signals is allowed to continue for all time, including every sunspot and every cosmic ray count rate and therefore all of the power ever produced by the signals. As k increases, so too does the frequency, which means the

time period of subsequent modes decreases by the inverse relationship with frequency. Smaller and smaller time periods results in less and less data being included in the signals per period, resulting in smaller amplitudes and less power for higher-frequency modes.

Additionally, notice that as k increases both power spectra no longer appear to have large, discernible peaks as they did for low k. Rather, both power spectra appear to level off for large k, becoming dominated by a highly oscillatory signal. The highly oscillatory nature of the signal for large k is due to high-frequency noise, which is unwanted for these measurements since the both data sets were taken over a 50 year period and tell us little about the overall nature of sunspot or cosmic ray cycles. We will return to this point in the optional section of the results.

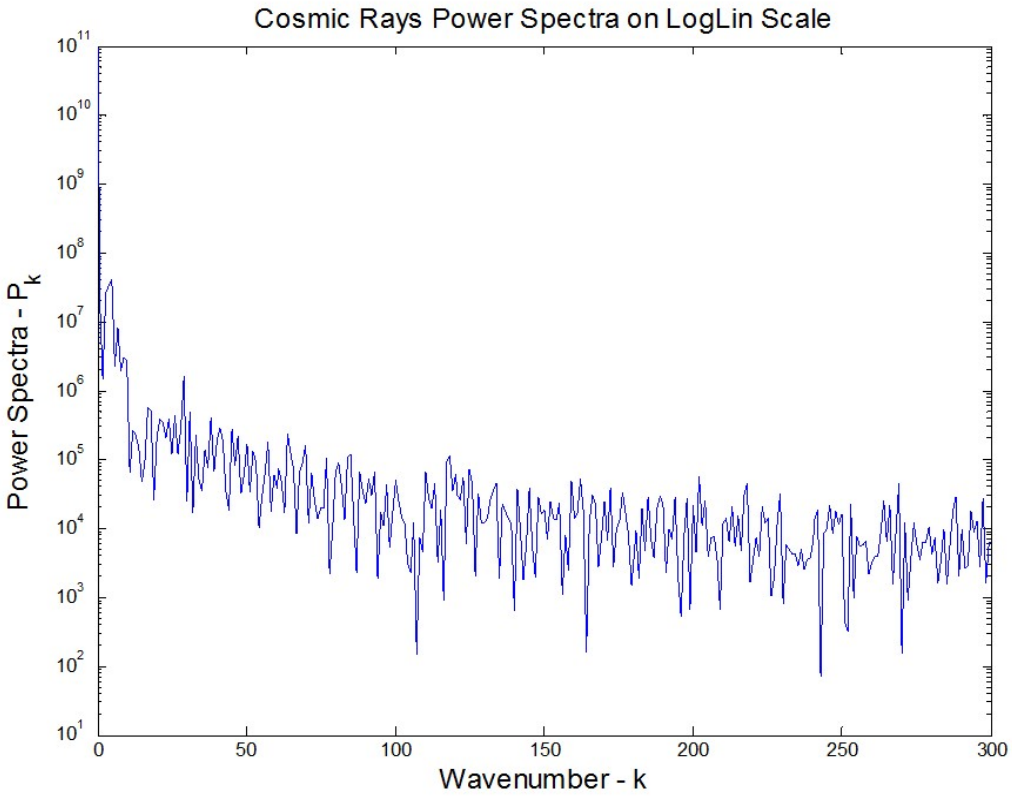

Figure 2: Cosmic rays signal power spectrum plot in k-space on a LogLin scale, meaning only the y-axis is on a logarithmic scale. Notice that, as for the sunspots, the largest non-zero spike occurs for a very low wavenumber k.

Though the dominant mode $k = 0$ gives us a qualitative understanding of the sunspot and cosmic ray signals, it tells us nothing about them in any practical or quantitative terms since the time period is infinite. Therefore, we wish to find the time period of the dominant non-zero mode for both signals. By looking at Fig. 1 and 2, we see that the second largest peaks occur for a very small k value, as expected. By zooming in on the peak in Fig. 1, we can find the k value of the dominant non-zero mode for the sunspots signal. This gives us Fig. 3 on the next page. From Fig. 3, we see that the dominant non-zero mode occurs at $k = 5$. By Eqn. (5), the dominant non-zero mode for the sunspots signal is for a frequency of $f = k/T = 5/50 = 0.1\ 1/year$. Therefore, the time period of the dominant non-zero mode for the sunspots signal is:

$$T_5 = 10 \quad years \tag{13}$$

By the same process, we can find the time-period of the dominant non-zero mode for the cosmic rays signal. Incidentally, we also find that dominant non-zero mode occurs at $k = 5$, meaning the

time period for the dominant non-zero mode of the cosmic rays signal is also given by:

$$T_5 = 10 \quad years \tag{14}$$

Thus, both the sunspot and cosmic ray signals appear to oscillate between their maximum and minimum amplitudes (with maximum power) for non-zero modes over a 10 year period.

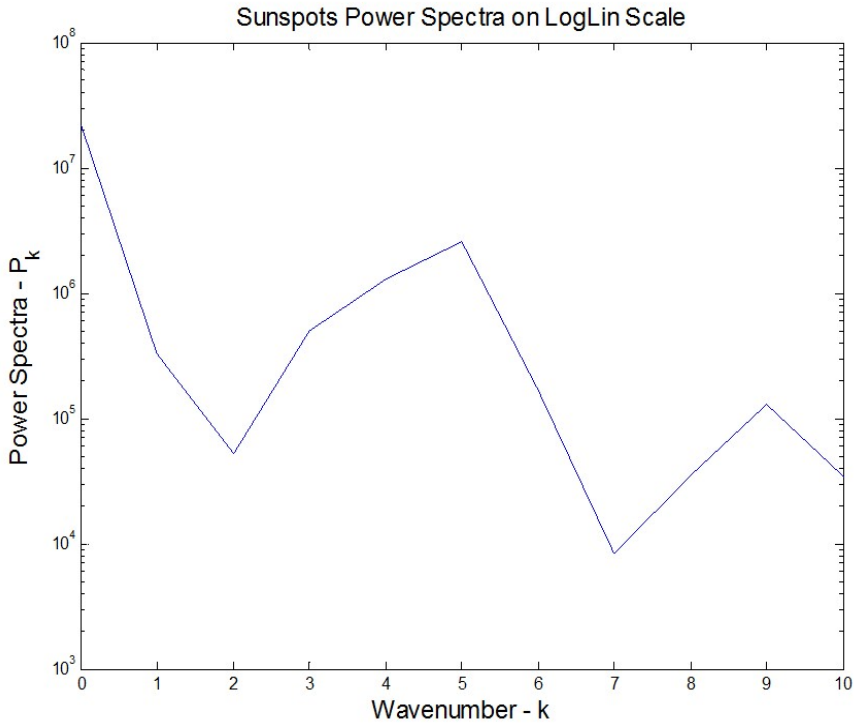

Figure 3: Sunspots signal power spectrum plot zoomed in on the dominant non-zero mode peak. Notice the dominant non-zero mode appears to occur for $k = 5$.

3.2 Normalized Autocorrelation Functions

In this section, we computed the normalized autocorrelation functions for both the sunspot and cosmic ray signals using the methods discussed in section 2. Recall that for a correlation function $C_{XY}(l(n))$, the autocorrelation function is the special case when $X = Y$, for signals X and Y. Also recall that the discrete correlation function is a function of a discrete time lag l, meaning that correlation function is in time-space. Thus the autocorrelation function measures how well a signal matches with itself after being shifted by a time lag l. The autocorrelation functions for the sunspot and cosmic ray signals are shown in Fig. 4 and 5 , respectively, on the following page.

As with the power spectra plots, we see many similarities between the normalized autocorrelation function plots of the sunspots signal and cosmic rays signal. Most notable is that both Fig. 4 and 5 have their maximum peaks for lag $l = 0$, where the value of the autocorrelation function is $C_{XX}(0) = 1$. This is a direct result of finding the *normalized* autocorrelation function o both signals. By first normalizing the signals using Eqn (12), we ensured that the autocorrelation function can only have values between -1 and 1. Thus the maximum value any normalized autocorrelation function can have is one, which indicates total or 100% correlation between the signals. With this understanding, we see that the normalized autocorrelation functions for the sunspot and cosmic ray signals should be one at $l = 0$ since this simply means that the signals equal themselves (have 100% correlation) when there is no time lag between the signal and itself.

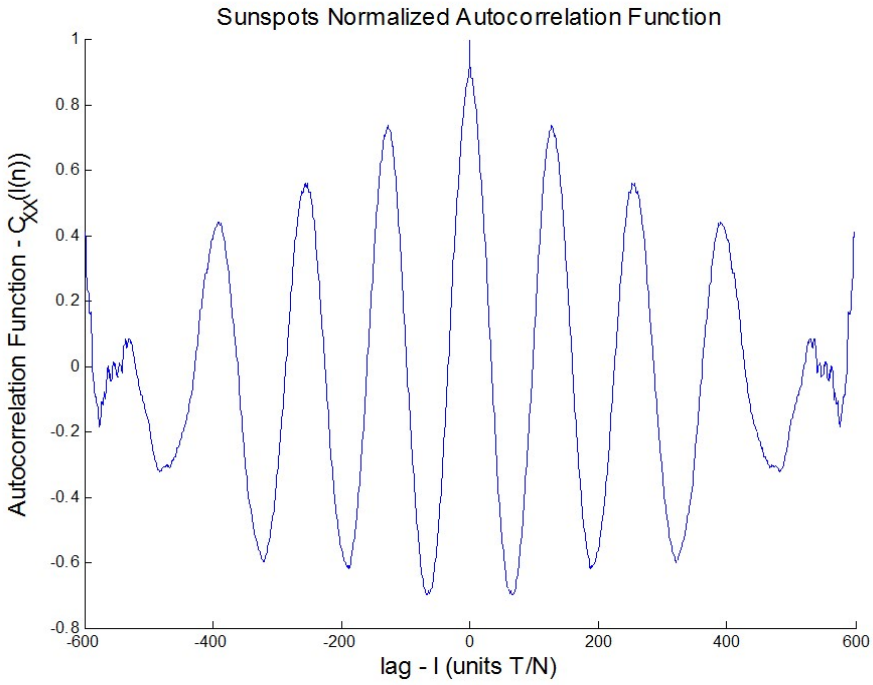

Figure 4: Sunspots signal normalized autocorrelation function. Notice that the maximum peak occurs at $l = 0$, where $C_{XX}(0) = 1$. This simply means that the sunspot signal matches itself 100% when there is no lag.

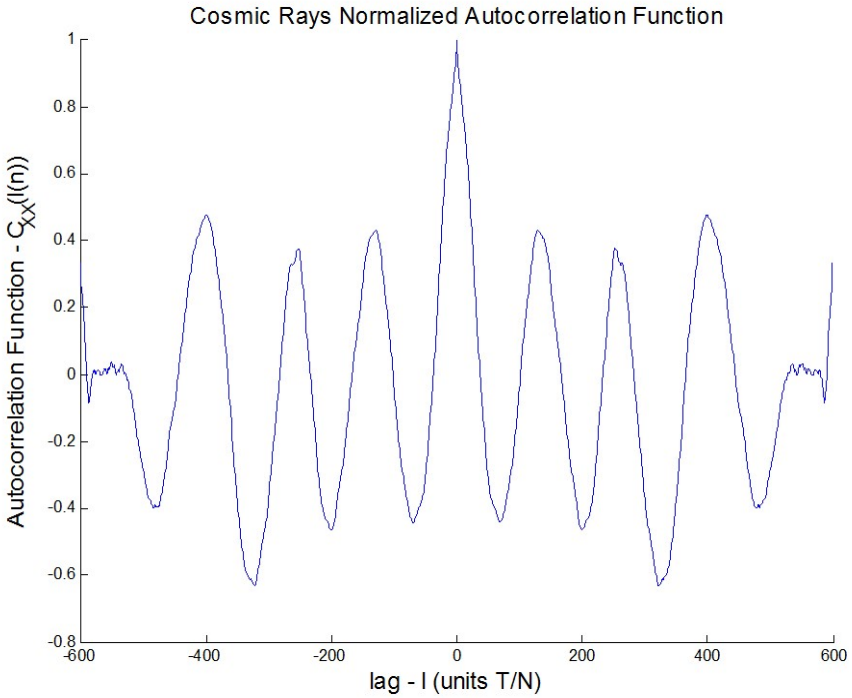

Figure 5: Cosmic ray signal normalized autocorrelation function. Notice that the maximum peak also occurs at $l = 0$, where $C_{XX}(0) = 1$. This simply means that the cosmic ray signal matches itself 100% when there is no lag.

Further similarities can be drawn between Fig. 4 and 5, such as the symmetry of the correlation functions about $l = 0$. This is another easily explained result: both the sunspot and cosmic ray signals are periodic, which is a required property in order to perform a Fourier transform of signal, therefore shifting a signal by the same time lag l forward or backward in time should produce the same decrease in correlation from the maximum at $l = 0$.

A difference between Fig. 4 and 5, however, is how quickly the autocorrelation functions decrease from one as $|l|$ is increased. For the sunspot autocorreletion function, the correlation drops from 1.0 at $l = 0$ to about 0.75, the next highest peak, at about $l = 130$. The cosmic ray autocorelation function, on the other hand, drops from 1.0 at $l = 0$ to about 0.4, which is also the next highest peak and also at a lag of about $l = 130$. This peak-to-peak lag difference is equivalent to one period or one sunspot or cosmic ray cycle. Therefore, the sunspot signal autocorrelation between itself and the next sunspot cycle only drops by 15% from its maximum whereas the cosmic ray signal autocorrelation between itself and the next cosmic ray cycle drops by 60% from its maximum.

This result can be interpreted as meaning that the sunspots signal, a measure of solar magnetic activity, strongly influences future solar magnetic cycles and is strongly influenced by past cycles, with the strongest correlation being between with nearest-neighbor cycle at 75% correlation. For every cycle beyond the nearest-neighbor cycle, however, the correlation steadily decreases to about 40% at the third cycle from $l = 0$. Thus, every current cycle of solar magnetic activity will strongly influence the next cycle, however that influence steadily decreases with each cycle. This makes sense physically because, for short periods of time, the Sun can be thought of as a relatively closed system (relative to the Universe), therefore we would expect current cycles of solar magnetic activity to strongly determine future cycles. The 15% drop in correlation from the current cycle to the next and the subsequent decline in correlation with future cycles can be attributed to the fact that the Sun is not in fact a closed system and after long periods of time, other solar activity such as the radiation emitted by the Sun begins to have an impact on future solar magnetic activity, meaning that current sunspot cycles alone do not wholly determine future ones.

The cosmic ray results can likewise be interpreted as meaning that a cosmic ray cycle weakly influences future cosmic ray cycles. Though a current cosmic ray cycle is correlated (not anti-correlated) with its nearest-neighbor cycle, it only has about 40% correlation, much less than for the sunspot cycles. This is due the fact that we were able to think of the Sun as a relatively closed system over short periods of time whereas the same assumption cannot be made of the source of cosmic rays: the Universe. Because the Universe is an open system, various phenomenon such as solar activity, magnetic field fluctuations in far away and neighboring planets, etc., can influence cosmic ray cycles. Therefore it is unlikely that a current cosmic ray cycle alone will be strongly correlated with future cycles, resulting in only 40% correlation with the nearest-neighbor cycle. Interestingly, while the correlation between the current cosmic ray cycle and the second cycle decreases further to about 35%, the third cycle sees an increase in correlation to about 50%. Evidently, a current cosmic ray cycle more strongly influences the third cosmic ray cycle than the first or second.

Finally, we mentioned earlier the time-period of a solar or cosmic ray cycle as being the peak-to-peak difference in the lag Δl of the autocorrelation functions. We know that the maximum peak for both autocorrelation functions occurs at $l = 0$. Therefore, by finding the l at which the next (or previous) peak occurs, we can determine the time-period of either cycle. We first determine the solar cycle time-period by zooming in on Fig. 4 around $l = 130$, where the next peak seems to occur. This gives us Fig. 6 on the next page. From Fig. 6, we see that the next peak occurs at $l = 128$, which means $\Delta l = 128$. By using the equation given in Eqn. (11) for l, we find the solar time-period T_S to be about:

$$T_S \approx 10.67 \quad years \tag{15}$$

By the same process, we can find the cosmic ray time-period T_C. we find the next peak occurs at $l = 129$, meaning $\Delta l = 129$. This gives us a cosmic ray cycle time-period of about:

$$T_C \approx 10.75 \quad years \tag{16}$$

Thus, the time-periods for both the solar sunspot and cosmic ray cycles are close but not quite the same. This means that both cycles overlap for a brief period of time. To analyze this further, we will find the cross-correlation function between the two signals.

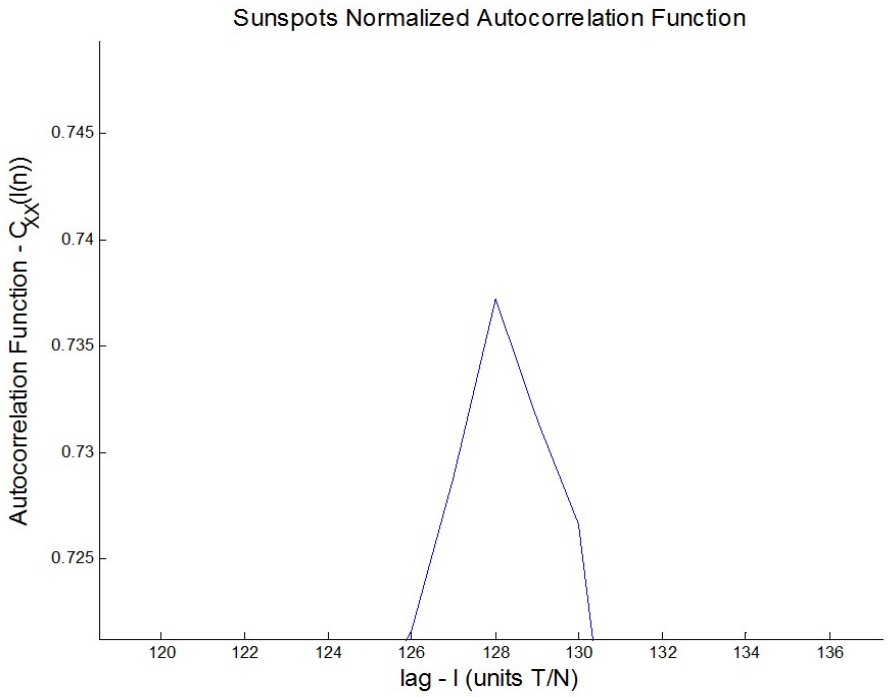

Figure 6: Sunspot signal normalized autocorrelation function zoomed in on the first peak from $l = 0$. Notice that this peak occurs at $l = 128$, which determines the period of the solar cycle.

3.3 Normalized Cross-Correlation Function

We once again use the correlation function defined in Eqn. (10), however this time we want to find the correlation between the sunspots signal and the cosmic rays signal, meaning $X \neq Y$ in the correlation function. Again, we normalize the data so our correlation function is bounded between -1 and 1. The cross-correlation function between the sunspot and cosmic ray signals is shown in Fig. 7 on the next page.

The most noticeable difference between the cross-correlation functions and the autocorrelation functions is the fact that a minimum occurs near $l = 0$ for the cross-correlation function whereas a maximum occurred at $l = 0$ for the autocorrelation function. Negative correlation values indicate anticorrelation, meaning that signals do not occur at the same time and do not match without lag. We expect this result for a cross-correlation function between solar sunspots and cosmic rays because during periods of increased solar magnetic activity, the stronger magnetic field deflects cosmic rays that are one their way to Earth. Thus, when the solar sunspots cycle is at a maximum, we expect the cosmic rays cycle to be near a minimum, leading to strong anti-correlation near zero lag.

At zero lag, the cross-correlation function has a value of

$$C_{XY}(0) = -0.789 \tag{17}$$

which was found in Python by search for the value $C_{XY}(l)$ when $l = 0$. While not totally anti-correlated, which occurs when $C_{XY}(l) = -1$, the cross-correlation function is still very strongly anti-correlated when there is no time lag between the sunspot signal and the cosmic ray signal. This means that despite the solar cycles preventing a large percentage of cosmic rays from reaching

Earth, they evidently do not stop all of the cosmic rays from reaching Earth. Additionally, recall from last problem the difference in time-period between the sunspot cycle and cosmic ray cycle. The fact that these time-periods are not exact guarantees that the two signals must correlate somewhat, again contributing to the anti-correlation only being 78.9%.

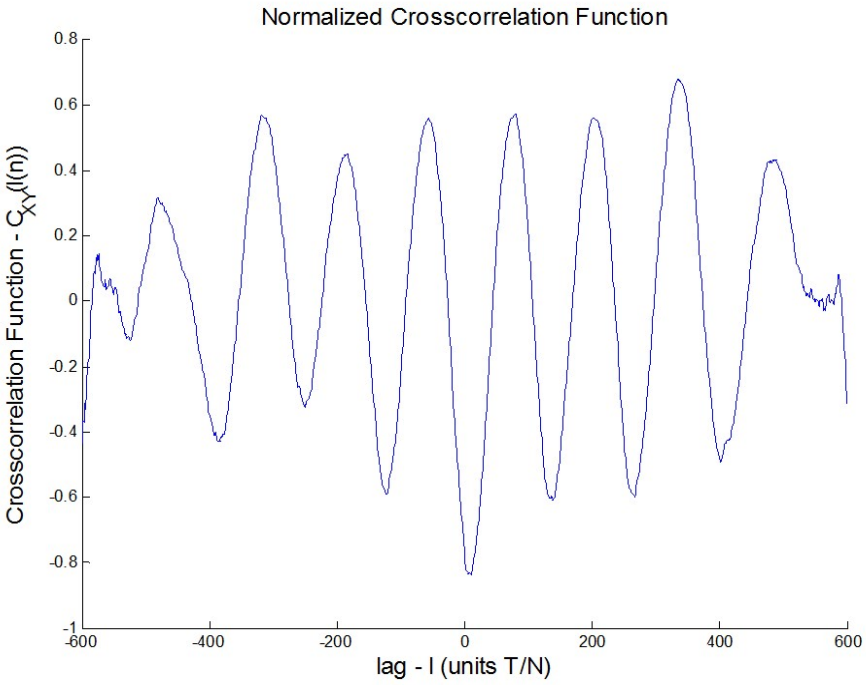

Figure 7: Cross-correlation function between the sunspot and cosmic ray signals. Notice how, unlike the autocorrelation functions, there is a minimum instead of a maximum and it occurs at $l = 10$ rather than at $l = 0$. Also notice that function is not symmetric about the minimum, also unlike the autocorrelation functions.

Another difference between Fig. 7 and Fig. 5 and 6 is if you look closely, you will notice that the absolute minimum of the cross-correlation does not occur at $l = 0$, as we would expect it to from out experience with the autocorrelation functions. Rather, the absolute minimum is shifted to positive lag value. We determined the l value at which the cross-correlation function is an absolute minimum by once again zooming in on the minimum peak. We found that the absolute minimum occurs at

$$l_{min} = 10 \tag{18}$$

with a cross-correlation value of

$$C_{XY}(10) = -0.838 \tag{19}$$

Even the absolute minimum of the cross-correlation function is not -1, meaning that the sunspots cycle and the cosmic ray cycles will never be entirely anti-correlated. Also important is that fact that the absolute minimum of the cross-correlation function occurs at $l = 10$, meaning that the two signals are only maximally anti-correlated when separated by a 1 *year* lag. This, in addition to the asymmetry of the cross-correlation function, is likely due to the difference in time-periods between the two signal cycles, as we showed in the last problem. Because the time-periods of the two cycles are not exactly the same, the cycles can never be completely out of phase and there must be some overlap between the sunspot cycle and the cosmic ray cycle. This illustrated best by the fact that the cross-correlation is not at an absolute minimum at $l = 0$, when there is no lag between

the two signals. Rather, some time must pass for one of cycles to completely end before maximum anti-correlation can be achieved.

For the cross-correlation of the sunspot and cosmic ray cycles, it is likely the sunspot cycle that must wait for the cosmic ray cycle to fully conclude before maximum anti-correlation can be achieved. This is because the period of the cosmic ray cycle was shown to be slightly longer than the sunspot cycle. This also makes sense physically because as the the sunspot cycle is beginning cosmic rays are still able to reach Earth since the magnetic field from solar activity is not yet strong enough to greatly deflect the cosmic radiation. The "charging up" of the magnetic field due to increased solar activity that is required before it is strong enough to deflect cosmic rays is therefore responsible for the longer cosmic ray cycle time-period, for the absolute minimum of the cross-correlation function occurring at $l = 10$, and for the failure of the two cycles to have an anti-correlation of $C_{XY}(l) = -1$.

3.4 Optional: Low-Pass Filter

For this section, we were to create a low-pass filter to remove the high-frequency noise of both the sunspot and cosmic ray signals. The unfiltered signals as a function of time are shown in Fig. 8 and 9 below. We can remove the noise from these signals through a fairly simply process. First, we must Fourier transform both data sets from the time domain into the frequency (k-space) domain. Next, we choose a maximum frequency f_{max} where keep all frequencies less than f_{max} and set equal to zero all frequencies greater than or equal to f_{max}, which is what makes this process a low pass filter since we only keep low frequency values. Finally, we Fourier transform the filtered frequency domain signals back to the time domain, giving us out low-pass filtered sunspot and cosmic ray signals.

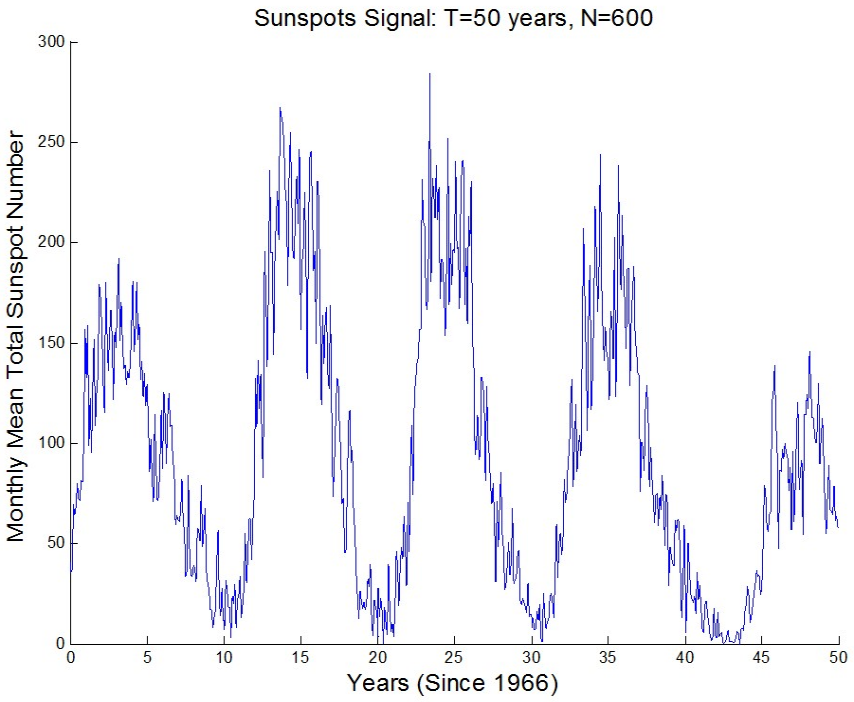

Figure 8: Unfiltered sunspot signal as a function of time in years. Notice the jagged, high-frequency oscillations, indicating noise.

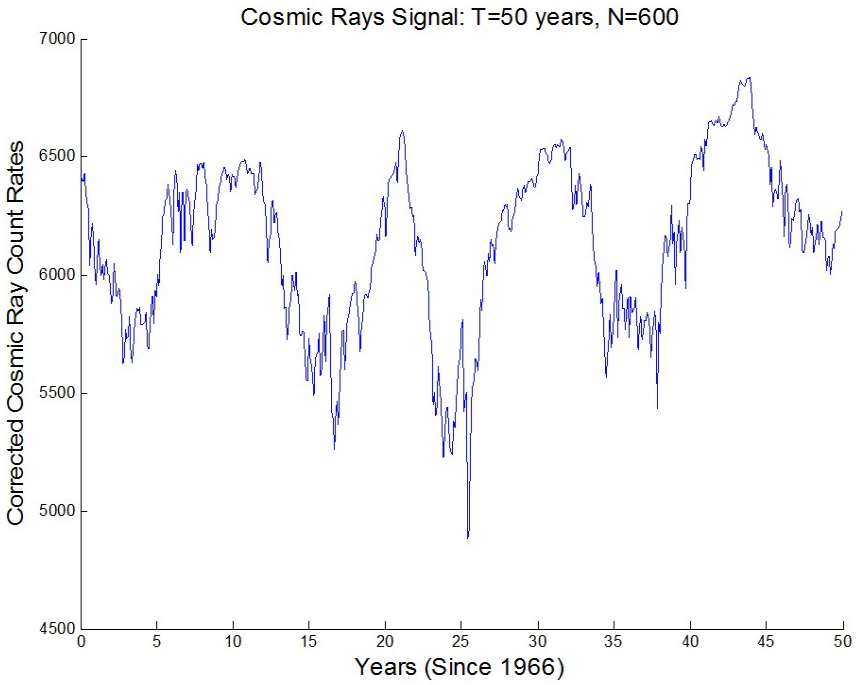

Figure 9: Unfiltered cosmic ray signal as a function of time in years. Notice how noisy the signal is.

Below we have plotted a few signals with different cut-off frequencies for both the sunspots signal and the cosmic rays signal in Fig. 10 and 11, respectively. Because we determined the time-period of a sunspot and cosmic ray cycle to be about 10 $years$, we started at either $f_{max} = 0$ or $f_{max} = 0.1$ and incremented the maximum frequency by 0.1.

First, let us inspect Fig. 10. In Fig. 10 we see that when $f_{max} = 0$, signals of all frequencies are filtered, resulting in a straight line at zero, as expected. For $f_{max} = 0.1$, the cut-off frequency is the frequency of the dominant non-zero mode, the mode that gives the single largest contribution to the amplitude and power of the sunspots signal. When $f_{max} = 0.1$, the sunspots signal is a clean, smooth signal with no high-frequency oscillations, however the amplitude of the signal is quite small since the dominant non-zero mode has been filtered out (barely). In fact, from the plot we can see that the sunspots signal even has periods greater than 10 $years$, as expected when we filter out frequencies greater than or equal to 0.1. As we increased the cut-off frequency to 0.2 we observe a large jump in the amplitude, since the dominant mode is no longer filtered out, and the sunspots signal takes it general shape. Increasing f_{max} further and high-frequency oscillations begin to appear near the peaks of the signal. These high-oscillations are the undesirable noise we wish to filter out, and if we let f_{max} increase to the maximum frequency of 6, then we simply reproduce Fig. 8 since no frequencies have been filtered out. The oscillations in Fig. 10 and how they are trying to conform to Fig. 8 can be shown more clearly in Fig. 12. In Fig. 12, we can see more clearly that the high-frequency oscillations do not begin until $f_{max} = 0.4$.

The discussion regarding Fig. 11 is virtually identical to that for Fig. 10. The best cleanest signal also occurs when $f_{max} = 0.2$ because it includes the dominant mode but does not yet include high frequency oscillations which do not occur until a higher frequency. In the case of the cosmic ray signal, however, high-frequency oscillations occur a lower frequency than for the sunspot signal. This is best shown in Fig. 13, where the high-frequency oscillations appear to begin as early as $f_{max} = 0.3$. Additional plots for large f_{max} for both signals are given to show that the signals eventually converge to Fig. 8 and 9 and the high-frequency oscillations are added.

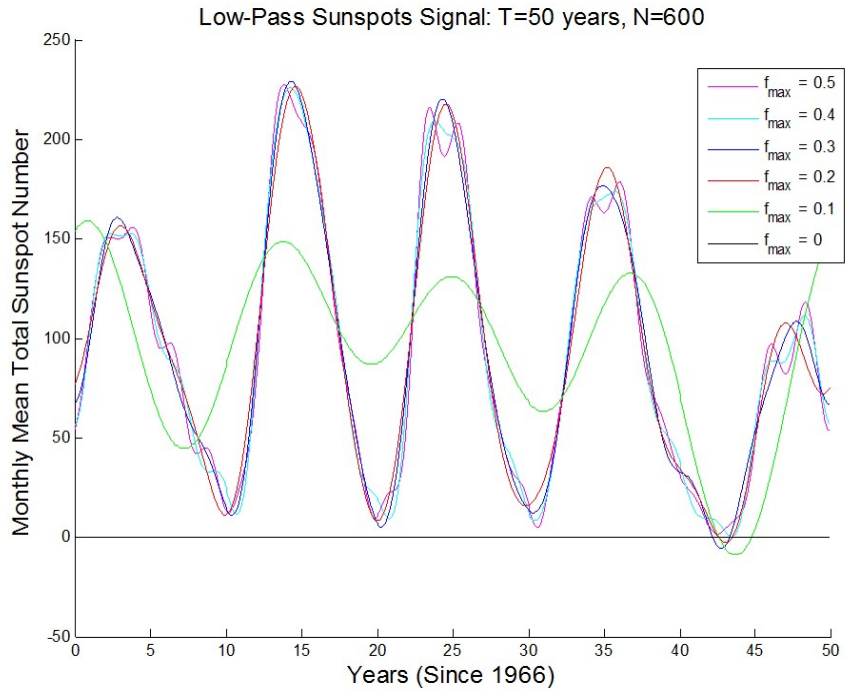

Figure 10: Filtered sunspot signal as a function of time in years for different cut-off frequencies f_{max}. Notice how more high-frequency oscillations are added at the extrema as f_{max} is increased.

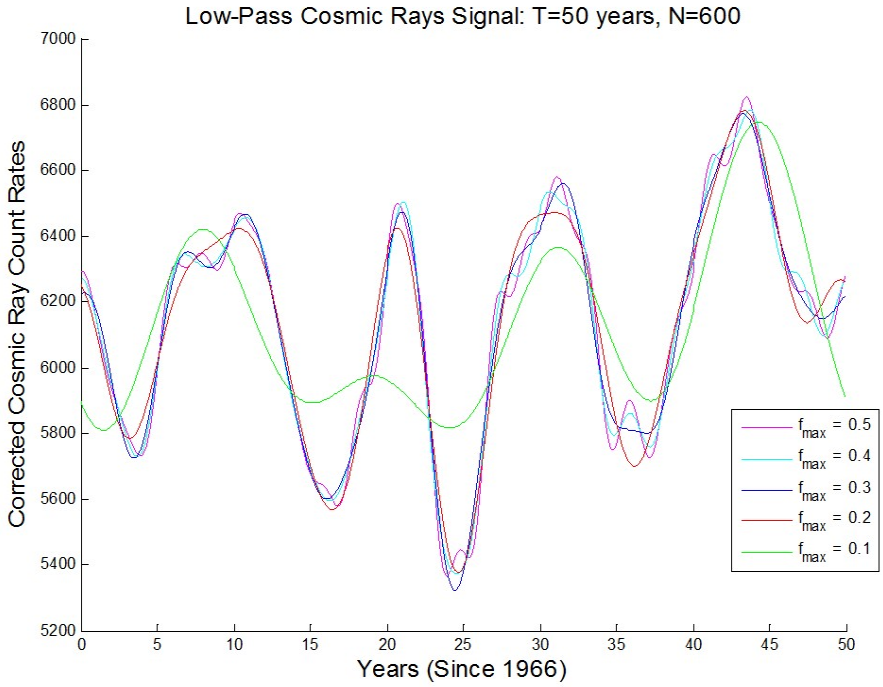

Figure 11: Filtered cosmic ray signal as a function of time in years for different cut-off frequencies f_{max}. Notice how more high-frequency oscillations are added at the extrema as f_{max} is increased.

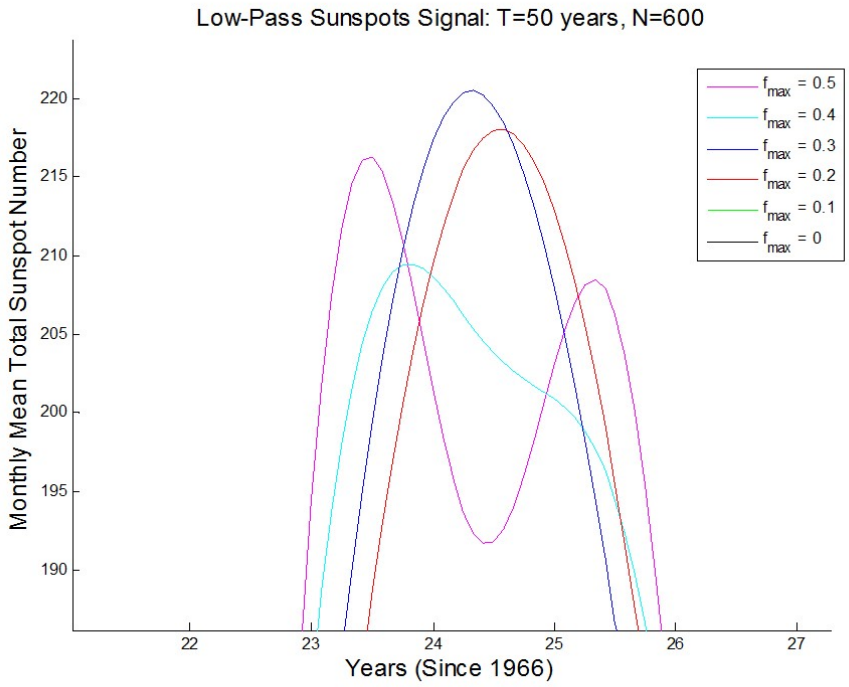

Figure 12: Zoomed in filtered sunspots signal as a function of time in years for different cut-off frequencies f_{max} about an arbitrary peak. Notice how high-frequency oscillations appear as f_{max} is increased, and how the extrema will eventually converge to Fig. 8 as $f_{max} \to 6$.

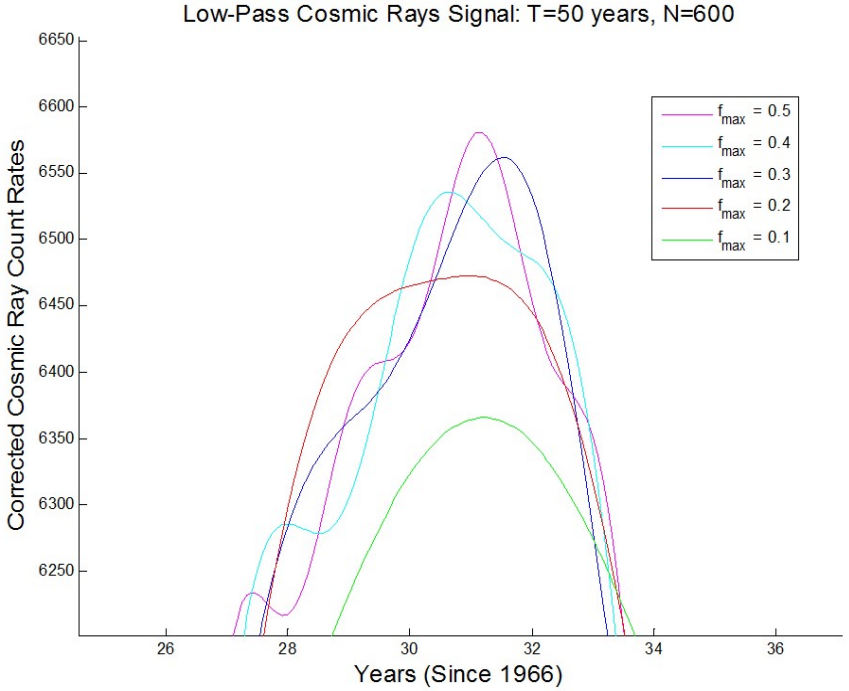

Figure 13: Zoomed in filtered cosmic ray signal as a function of time in years for different cut-off frequencies f_{max} about an arbitrary peak. Comparing this figure to Fig. 12, we notice that the cosmic ray signal has much more high-frequency oscillations for lower f_{max} than the sunspot signal.

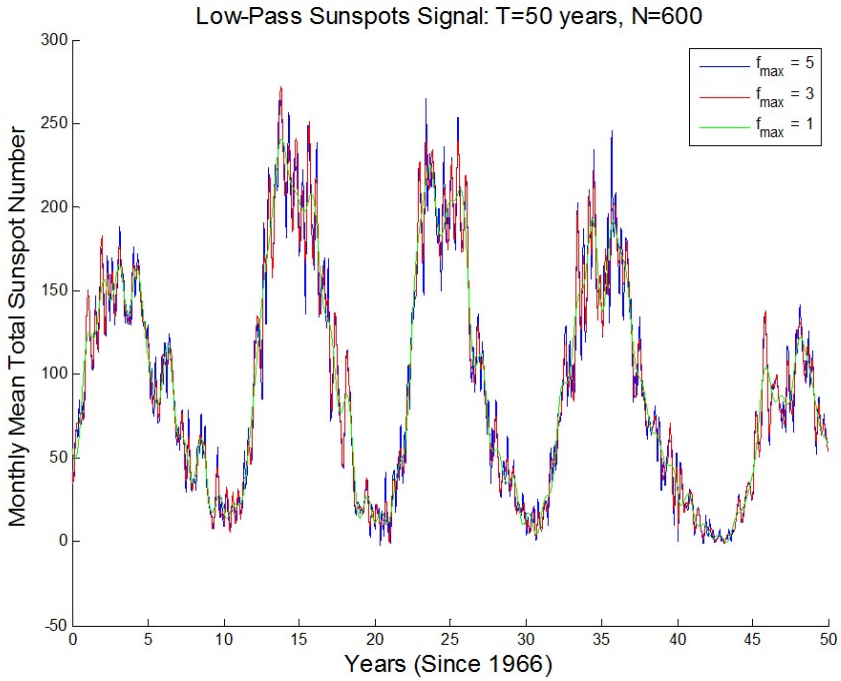

Figure 14: Filtered sunspot signal as a function of time in years for different, large cut-off frequencies f_{max}. Notice how high-frequency oscillations appear and f_{max} is increased the figure eventually becomes Fig. 8.

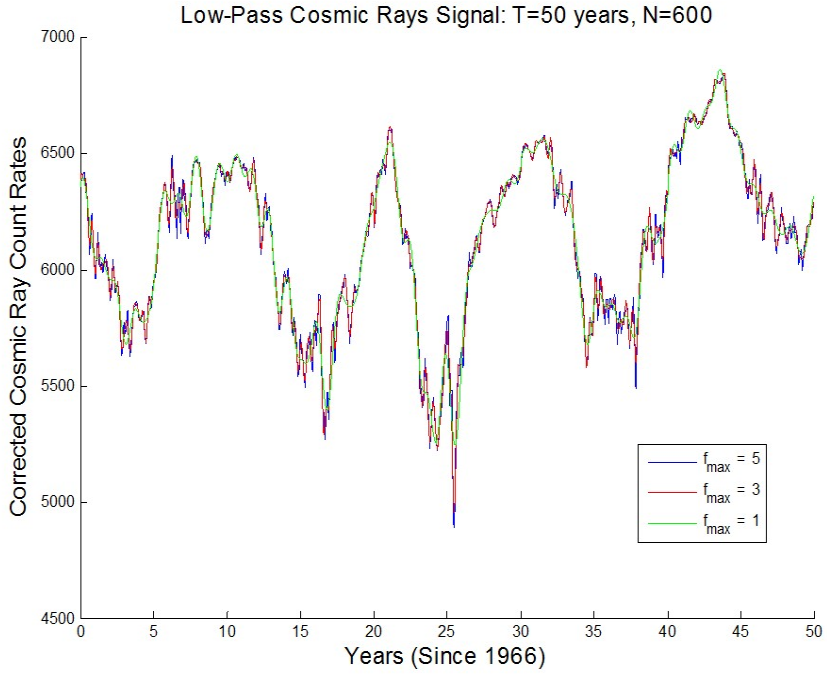

Figure 15: Filtered cosmic ray signal as a function of time in years for different, large cut-off frequencies f_{max}. Notice how high-frequency oscillations appear and f_{max} is increased the figure eventually becomes Fig. 9.